Journal of Magnetism and Magnetic Materials 444 (2017) 354–360

Contents lists available at ScienceDirect

Journal of Magnetism and Magnetic Materials

journal homepage: www.elsevier.com/locate/jmmm

Research articles

# Dual-cantilever magnetometer for study of magnetic interactions between patterned permalloy microstructures

K. Neilinger *, J. Šoltýs, M. Mruczkiewicz, J. Dérer, V. Cambel

*Institute of Electrical Engineering, SAS, Dúbravská cesta 9, 841 04 Bratislava, Slovakia*

ARTICLE INFO

*Article history:*
Received 29 March 2017
Received in revised form 16 August 2017
Accepted 19 August 2017
Available online 20 August 2017

*Keywords:*
Cantilever magnetometry
AFM cantilever
MFM
Micromagnetic simulations
Permalloy ellipses

ABSTRACT

We have designed and implemented a dual-cantilever magnetometer, in which the coupling magnetic forces between the two cantilevers can be switched on/off by an external magnetic field. The coupling is realized by a pair of ferromagnetic ellipses, located on the cantilevers. One of the ellipses is "narrow" – it bears only a single domain magnetic state independently of the applied external field. The other one is "wide", and can be either in single- or closure-domain states depending on the applied field. In such configuration, the interacting force between the cantilevers can be attractive (both ellipses are in single domain state conforming to the external field), repulsive (both are in single domain states, but the narrow ellipse is in a meta-stable state, with magnetization opposite to the field) or switched off (when the closure domain state appears in the wide ellipse). We found that the coupling between the ellipses directly corresponds to the phase shift of the vibrating cantilevers. In this manner, the cantilever phase detection can be used to read out the magnetic state of the ellipses, which depends on the applied magnetic field. Moreover, we study how the magnetic state of the wide ellipse influences the flipping field of the narrow ellipse. Our observations are supported by micromagnetic simulations and by additional magnetic force microscopy experiments. We also discuss sensitivity and potential application of the magnetometer in future experiments.



## 1. Introduction

The magnetic sensing at micro- and nano-scale is important from both fundamental and practical standpoints. Thus, there is an increasing need for techniques that can reliably detect the weak magnetic signal coming from the low dimensional magnetic structures. Additionally, it is preferable to use a detecting method that does not perturb the magnetic state of the inspected system. These requirements can be fulfilled by micromechanical magnetometers, which uses sensitive cantilever. The cantilever magnetometry covers wide range of applications. They were used, for example, for studying the behavior of the magnetization reversal and magnetic moment of ferromagnetic thin films [1,2] or to evaluate the effect of magnet size and shape on magnetic properties [3,4]. Cantilever magnetometry was also used in the field of superconductivity, for example, for studying the vortex lattice melting of superconducting $NbSe_2$ [5], vortices in mesoscopic $Sr_2RuO_4$ rings [6] and persistent currents in mesoscopic normal metal rings [7]. The sensitivity has been constantly improved thanks to the advances in fabrication of ultrasensitive cantilevers. As a result, magnetometers with ultimate force sensitivity in the range of attonewton were developed [8,9].

Standardly, magnetic samples are carefully attached or lithographically defined on the cantilever and experiments are based on measuring cantilever's response (deflection, torsion, or shift in resonant frequency) as a function of applied magnetic field. This response results from the magnetic torque produced by the sample magnetization when subjected to external magnetic field. The torque is then transmitted to the cantilever. In most cases, cantilever contains one single magnetic element or large arrays of uniform elements (to achieve higher overall sensitivity). In the case of arrays, the inter-element separation is set large enough to avoid interactions between neighboring elements. Thus, the array response is influenced only by the outer applied field. It would be also interesting to use cantilever magnetometry to study mutual interactions between the magnetic elements. The interactions become more dominant when the edge-to-edge gap is smaller than element lateral size. Understanding these interactions is essential to the development of magnetic memories [10], field sensors [11] or logic devices [12].

There have been a number of studies dealing with the interaction of micro- or sub-micrometer-sized elements, however, all of them were performed by other techniques rather than by can-

* Corresponding author.
*E-mail address:* katarina.neilinger@savba.sk (K. Neilinger).

http://dx.doi.org/10.1016/j.jmmm.2017.08.055
0304-8853/

tilever magnetometry [13–16]. Up to now, only a few experiments have been reported based on this concept [17,18]. Gao et al. published pioneering work in this field, in which paired $Ni_{80}Fe_{20}$ bars on sensitive microcantilever were prepared and they studied the magnetization reversal loops of these bars. Obtained hysteresis curves showed a series of stable switching states which was related to the domain wall motion in the bars. Gao's concept was characterized by high sensitivity thanks to three conditions: first, the special cantilever was designed with extremely low spring constant; second, the high quality factor of the cantilever was achieved by measurement in vacuum; third, eight identical pairs of bars were defined on the cantilever to get higher signal. The last parameter can introduce statistical variations of switching field because each bar may have a different reversal field due to different defect structures formed during the focused ion beam (FIB) processing.

Here we present cantilever magnetometer by which we can measure mutual interactions of one pair of ferromagnetic elements. Magnetometer was prepared by modification of commercial atomic force microscopy (AFM) cantilever. Thanks to standardized chip dimensions, the detection can be performed by common AFM head and there is no need for special interferometric equipment. The concept is based on measuring mutual interaction between two cantilevers with ferromagnetic ellipses located on each of them. So in this case we do not measure torque as it is usual in standard cantilever magnetometry, but the coupling forces between cantilevers. These interacting forces are larger than torque, thus we do not need to use specialized low-spring cantilever and vacuum conditions. We measure the phase shift of dual-cantilever in the applied external magnetic field which corresponds to change of magnetic states of ellipses. Obtained phase shift curve was correlated with micromagnetic simulations using the MuMax3 software package [19]. We also mapped the magnetic signal over the similar ellipses fabricated on a flat substrate by magnetic force microscopy (MFM). This experimental results and numerical simulation allowed for precise interpretation of the observed phase shift signal.

## 2. Dual-cantilever magnetometer design and fabrication

In this section, we propose the design of the dual-cantilever magnetometer. It is based on two parallel cantilevers located very close to each other, which can magnetically interact by magnetic microelements located on their free ends. Mutual interaction depends on the magnetic state of each of the element and can be controlled by external magnetic in-plane field. Schematic sketch of the dual-cantilever magnetometer can be seen in the Fig. 1. Magnetic microelements are represented by permalloy ellipses, with several stable magnetic states possible in the external magnetic field [20]. The magnetic states depend on the length-to-width aspect ratio (LTW) of the ellipses and their overall dimensions [21–23]. In our design, we used one ellipse "narrow" with higher length-to-width ratio (LTW > 4) and second one "wide" with small ratio (LTW < 3).

The narrow ellipse is always in a single-domain magnetic state independently on the external field applied, while the wide one can bear also a vortex state configuration (at small external fields [21]). When applying sufficiently high external magnetic field along the major axis of ellipses, single domain states are introduced in both of the ellipses. When the field is lowered and reversed, various magnetic states are introduced to the wider ellipse, first vortex then single domain state, respectively. The initial single domain state in narrow ellipse remains until high field with opposite sign is applied due to high LTW ratio [21,23]. The possible states that can stabilize when magnetic field is varied are presented in the inset of the Fig. 1. The changes in the magnetization of the ellipses depending on the external magnetic field are measured by phase detection, which measures the cantilever's phase of oscillation relative to that of the piezo drive.

For the fabrication of the dual-cantilever magnetometer, we used commercial silicon tipless AFM cantilever with spring constant of ~9 N/m [24]. The 40 nm thin layer of magnetic material Permalloy ($Ni_{80}Fe_{20}$) was deposited on cantilever using evaporation by electron beam. Then, FIB workstation FEI Quanta 3D using a $Ga^+$ liquid metal ion source was used to cut cantilever into two longitudinal parts and to pattern ellipses on them by FIB milling. Fabricated cantilevers are shown in the Fig. 2. Size of the narrow ellipse was $2.5 \times 14\ \mu m^2$ (LTW = 5.6). Size of the wide ellipse was $7.5 \times 4\ \mu m^2$ (LTW ~ 1.8). Final dual-cantilever was 98 μm long, 36 μm wide, with thickness of 1.4 μm. The lateral and vertical distances between the edges of magnetic ellipses were 450 nm and 110 nm, respectively. The vertical distance plays a crucial role in our concept – $z$ component of the magnetic interaction between the ellipses represents the coupling force between the cantilevers.

## 3. Experiment

All experiments were carried out in AFM microscope (Ntegra Prima, NT-MDT). The chip with prepared dual-cantilever magnetometer was inserted into the measuring head. The cantilever's phase was measured by PSD detector and processed by AFM control software. Laser beam spot was large enough to illuminate both cantilevers. In this case, the frequency spectrum of dual-cantilever

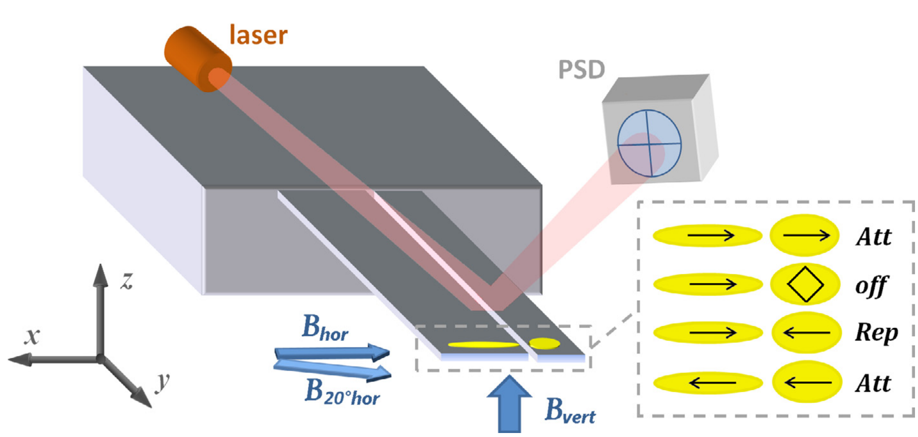


**Fig. 1.** Schematic representation of the experimental setup. Possible magnetic states of ellipses (single domain, vortex) are shown in the inset. According to them, mutual forces between cantilevers can be attractive (Att), repulsive (Rep) or switched off (off).

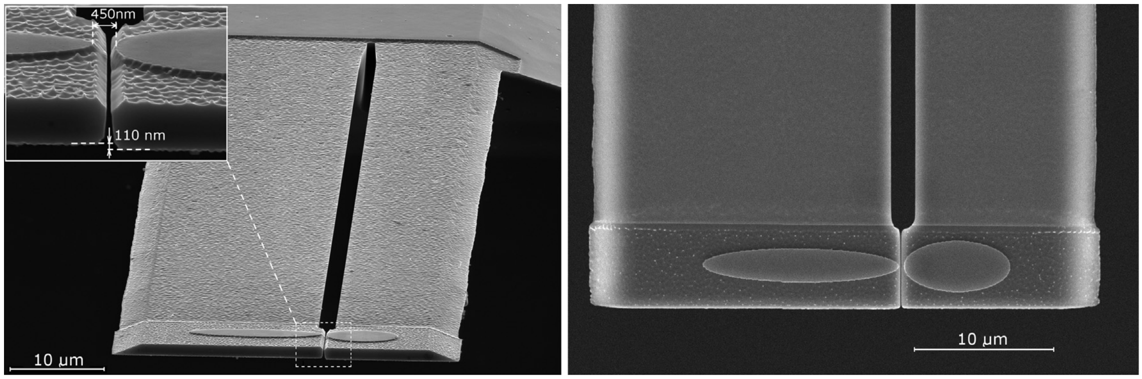


**Fig. 2.** Dual-cantilever with permalloy elliptical structures. Left: entire. Right: top view on prepared ellipses. The inset shows the distance between the ellipses and vertical separation of cantilevers.

system was characterized by two resonance peaks (~145 kHz and ~147 kHz), which corresponded to resonant frequencies of the individual cantilevers, oscillating in $z$ direction. Here we present measurements at 147 kHz, at which oscillates the cantilever with the narrow ellipse. It has to be stressed, that in our experiments only one of the cantilevers vibrates.

Since the cantilevers are oscillating in $z$ direction, z-component of the force generated by the interacting ellipses ($F_z$) produces a variation in a shift in the phase $\Delta\varphi$ of the oscillation of the cantilever given by [25]:

$$\Delta\varphi = \frac{Q}{k}\left(\frac{\partial F_Z}{\partial z}\right) \tag{1}$$

where $Q$ is the quality factor of the cantilever and $k$ is the cantilever spring constant.

The phase shift signal (see Fig. 3) reflects changes in force due to magnetic interactions between the narrow and the wide ellipse. We have found that the phase shift is independent on used resonant frequency (which of the cantilevers is vibrating).

The amplitude of the oscillations was set to 100 nm (amplitude of the second cantilever is zero), which means that the peak-to-peak distance of the ellipses varies from almost zero to 200 nm. All measurements were performed at ambient conditions.

If the phase signal has to be correlated with the magnetic states of the ellipses, we have to change their magnetic states and observe induced changes in the phase signal.

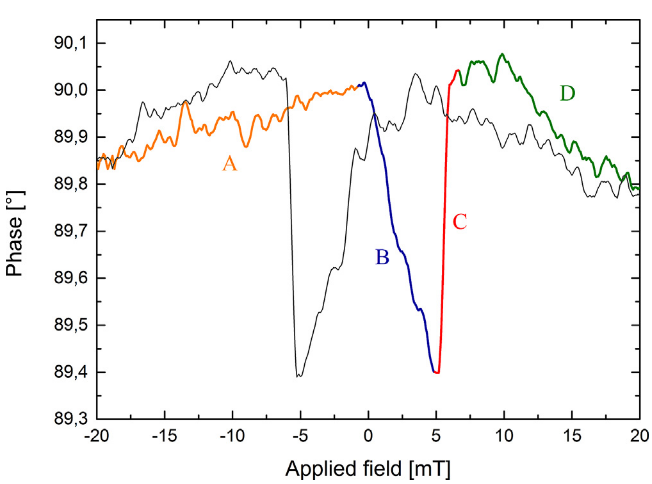


**Fig. 3.** Phase shift of dual-cantilever measured at frequency of 147,5 kHz detected by PSD detector.

The magnetic states in ellipses were changed by the external field applied to the system. Therefore, in the experiments we performed three different configurations of the external field.

## 4. Results and discussion

In the configuration described in the Fig. 1, the coupling between the cantilevers depends on the magnetic state of the ellipses. The force between the ellipses can be attractive, as well as repulsive (when both ellipses are in the single-domain state of the same or opposite orientation, resp.). Moreover, the interaction can be switched off, when the closure domain state with vortices appears in the wide ellipse. The black marks in the inset of Fig. 1 show four possible magnetic states. In this sense, our dual-cantilever magnetometer differs from other systems with magnetic particles located on cantilevers [7,17]. Those systems evaluate magnetic torque in external magnetic field, while the response (phase) of the presented dual-cantilever magnetometer reflects direct magnetic coupling between the cantilevers.

To change the magnetic state of the ellipses, and, consequently, the magnetic coupling between the cantilevers, we have studied magnetization reversal loops of the system in sweeping external magnetic field ($B_{hor}$ or $B_{20°hor}$). A typical loop is shown in the Fig. 3. Observed jumps on the curves reflect changes in the phase signal of the cantilevers, which correspond to notable changes of the magnetization state of the ellipses, e.g. for closure-domain state nucleation, single-domain state nucleation, or single-domain state flipping.

Graph presented in the Fig. 3 consists of two parts. The gray part corresponds to the field sweeping from positive to negative values, whereas colored part corresponds to the sweeping from negative to positive field values. For vivid illustration, this part is further divided into four segments of different color, marked as A, B, C, and D. The segment A (orange curve) and the segment D (green curve) correspond to single domain states in both ellipses with magnetizations oriented in the direction of the external field. The segment B (blue curve) reflects rapid changes of the magnetization of the wide ellipse. The segment C (red curve) shows the major change of the phase shift, which corresponds to the flipping of the single domain state in the narrow ellipse.

To illustrate and explain better the observed phase shift dependence of the dual-cantilever magnetometer, we have provided additional MFM experiments with two in-plane ellipses in external magnetic field (<±5 mT) applied in parallel with their long axes (Fig. 4). The magnetization reversal loop for the system with two ellipses was calculated using micromagnetic simulations for 5-times smaller system (package MuMax3, Figs. 5 and 6) [19]. Images

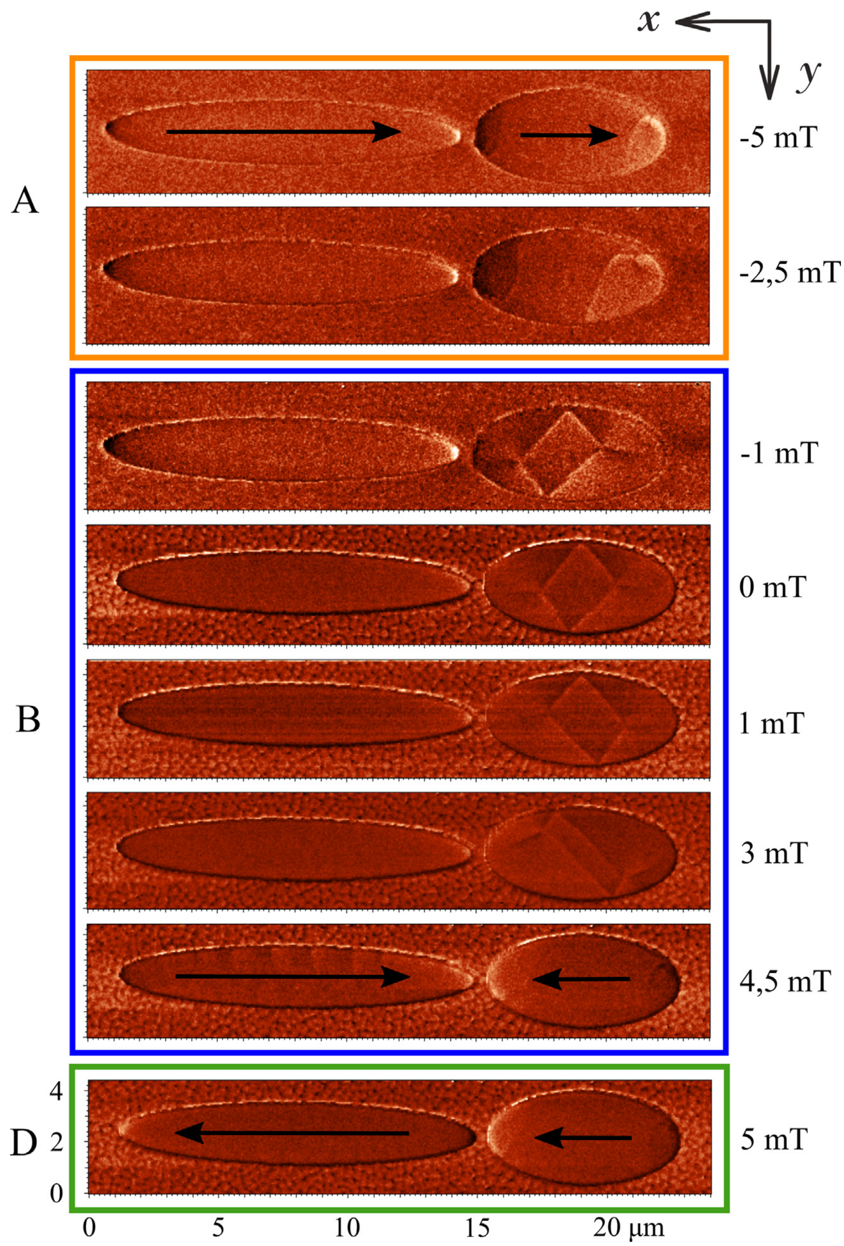


**Fig. 4.** MFM scans of ellipses on planar substrate measured in external magnetic field (value of the field is indicated on the right). Black arrows correspond to single domain states. Colored frames and letters indicate segments of the phase shift curve shown in the Fig. 3. (For interpretation of the references to colour in this figure legend, the reader is referred to the web version of this article.)

proportional to the MFM contrast were calculated for tip distance 20 nm (Fig. 6).

Now we discuss the supporting MFM experiments (Fig. 4) and simulations (Fig. 5) to explain the correlation between the magnetic states of the ellipses with the phase shift loop (Fig. 3).

First, we apply external magnetic field of the value of −80 mT to set both of the ellipses into the single-domain state. In this state, they are coupled by attractive magnetic forces. Then, the field is increased.

From −5 mT to −2.5 mT the ellipses still keep the single-domain state (state A in the Figs. 3 and 4). At −1 mT the closure-domain state with four vortices appears in the wide ellipse – two vortices are located in the central position and two of them at the ellipse edge (Fig. 4, third line). This fact lowers the interaction between the ellipses drastically, although the narrow ellipse remains in the single-domain state. This state remains up to +3 mT (Fig. 4, B), just the position of the vortices depends on the applied field (corresponding segment is still B in the Fig. 3).

At +4.5 mT the wide ellipse shows again single-domain state conforming to the external field. The transition from the closure-domain state to the single-domain state is represented by small jump in segment B in the Figs. 3, 5). The narrow ellipse still remains in the single-domain state oriented opposite to the external field (Fig. 4, 7th line).

Further field increase to +5 mT flips the magnetic moment of the narrow ellipse to opposite direction, which is represented by the large jump in the phase signal (Fig. 3, segment C). For higher fields, the attractive coupling between the cantilevers is again established (segment D in the Figs. 3, 5).

The magnetic field, at which the narrow ellipse switches, depends on the external magnetic field and on the field generated by the wide ellipse. The switching field of the narrow ellipse can

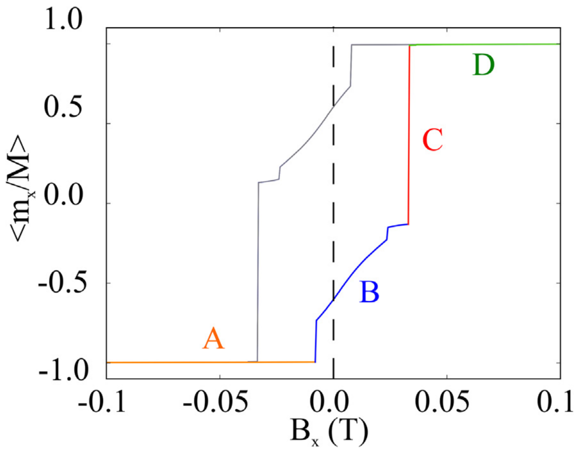


**Fig. 5.** Simulated magnetic hysteresis loop of the paired ellipses. Colored parts correspond to segments in the Fig. 3. (For interpretation of the references to colour in this figure legend, the reader is referred to the web version of this article.)

thus be precisely tuned by the magnetic state of the wide ellipse, polarity and locations of the pinned vortices, etc. And, vice-versa, the shift of the switching field of the narrow ellipse documents the change of the magnetic state of the wide ellipse. In this sense, the narrow ellipse probes the magnetic state of the wide ellipse.

Now we show that the dual-cantilever magnetometer is sensitive enough to distinguish the polarity of the vortices in the wide ellipse. To support this idea, we have repeated the magnetization reversal loops 100 times with external magnetic field sweeping from −80 mT to +80 mT, and with the field step 0.05 mT.

The experiment was carried out for 3 basic configurations of the dual-cantilever according the external magnetic field. In the first one, the external field was applied in parallel with the long axes of the ellipses ($x$ direction). In the second case, the sample was turned in the $xy$ plane in ~20 deg. The sense of the sample rotation is to control better the nucleation of the closure-domain state in the wide ellipse [26–28].

In the third case, the sample was turned in the $xy$ plane in ~20 deg and we have added constant vertical magnetic field ($B_{vert}$ = 3 mT) perpendicular to the sweeping magnetic field in order to control the polarity of the vortices in the wide ellipse. Our MFM simulations support this idea. Fig. 6(a) depicts magnetic state of the ellipses during the loop without $B_{vert}$ field – nucleated were two vortices with positive and two with negative polarities (recognized by white and black spots at vortex locations). After application of the $B_{vert}$ field during the magnetization loop, all vortex polarities were established into the same orientation (black spots only).

In the Fig. 7 we show graph of the collected data on the phase jumps. It depicts the number of phase jumps that correspond to switching field of the narrow ellipse in dependence of the field. Results are showed for the positive polarity of the switching field and positive constant field $B_{vert}$; results with opposite polarities are similar. From the Fig. 7 it is clear that when the field is applied in parallel with the long axes of the ellipses (in the $x$ direction), the characteristic is broad (standard deviation of the blue Gaussian approximation, $\sigma \sim 0.3$ mT), the narrow ellipse switches at several field values. This can be explained by variety of possible magnetic states in the wide ellipse (local chiralities/magnetizations, vortex polarities, etc.).

Now we turn the sample in the $xy$ plane in 20 deg and apply the sweeping field (Fig. 7, red part). Two changes in the distribution are observed: a) phase jumps occur at higher fields – this is because the corresponding $x$ component of the field is lower; b) the distribution shows two sharp maxima with $\sigma < 0.1$ mT – angle of 20 deg reduces the number of possible states in the wide ellipse [26–28]. We think that the two peaks correspond to two possible vortex polarities pinned in the wide ellipse close to the narrow ellipse.

If we now switch on small field $B_{vert}$ = +3 mT, only one very sharp peak is obtained ($\sigma < 0.1$ mT, black curve in the Fig. 7) because only one polarity of the vortex core is possible. The switching field is probably increased because the additional $B_{vert}$ field lowers the interaction force between the ellipses – a part of the force lines is coupled to the poles of the $B_{vert}$ field.

To summarize this part, we have shown how the phase shift signal correlates with the magnetic state of the ellipses in the dual-cantilever system. Advantage of the tested magnetometer is its high sensitivity – we have shown that the phase shift signal is sensitive to vortex polarity only.

In the case of magnetometer, magnetic objects are placed directly onto the cantilevers. Such magnetometer can be used also to study vortex dynamics in one of the magnetic objects. The basic configuration of the experiment should be similar to the one described in this paper. On one of the cantilevers is the object explored, and the second one serves as the "probe" – it contains for example ellipse in the single domain state which is not changing during the experiment. The external field is selected close to the value at which a dynamic process (switching to ground state) in the explored object should start in reasonable time. If the relaxation starts, interaction between the cantilevers will change, and the phase signal will change too. Such experiment would be useful for the study of vortex nucleation/annihilation processes, including

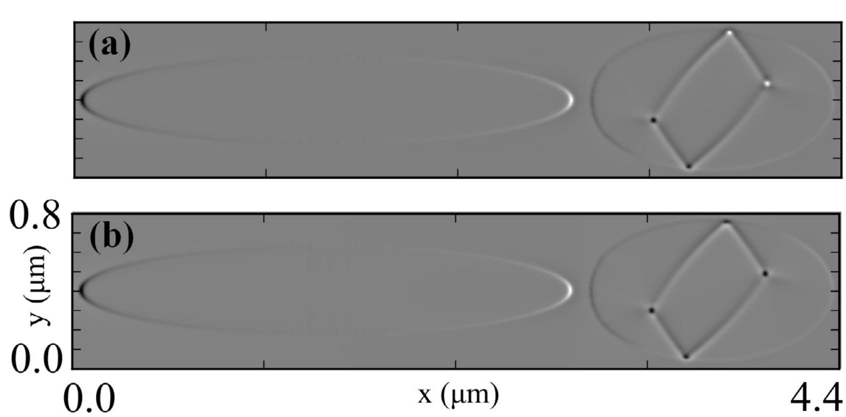


**Fig. 6.** Modeled MFM simulation without (a) and with (b) constant vertical field 3 mT. Black spots in wide ellipse represent the same polarity of all nucleated vortices (b).

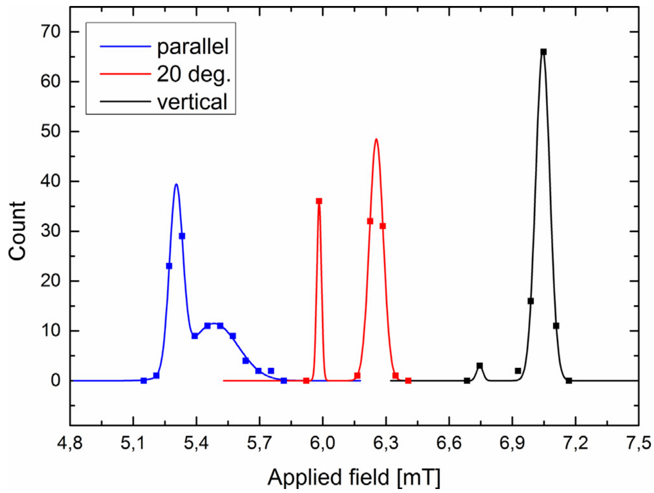


**Fig. 7.** Number of appearances of the switching field for the narrow ellipse in dependence of applied field. Lines represent Gaussian approximation and dots represent collected data. Blue curve – external field is parallel with the long axis of ellipses and $B_{vert}$ = 0 mT, red curve – applied field $B_{20°hor}$ and $B_{vert}$ = 0 mT, black curve – the same like red one but $B_{vert}$ = 3 mT. (For interpretation of the references to colour in this figure legend, the reader is referred to the web version of this article.)

its temperature dependence. Such experiments are over the scope of this paper, and represent next goal of our work.

Finally, we discuss how the sensitivity of the dual-cantilever can be improved in order to detect changes in nanosize structures. At first, it is important to note that the detected signal to noise ratio (Fig. 3) is high and smaller structures could be measured without modification of the present experimental setup. Additionally, according to the Eq. (1), the phase shift is inversely proportional to the cantilever spring constant $k$ and proportional to quality factor $Q$. Experiments described in this paper were realized at ambient conditions using standard probes with relatively high force constant (~9 N/m). The sensitivity can be increased by using cantilever with lower spring constant. Probes with 1–2 orders of magnitude lower spring constant are available commercially. However, low spring constant cantilevers suffer from poor quality factor $Q$. Then, to keep the quality $Q$ of the cantilever, the experiments has to be realized in corresponding vacuum [29,30]. Optimum value of the spring constant should be found according to the thermal and pink noise (1/f) of the realized experimental setup.

The Eq. (1) is also proportional to the gradient of the force. Decrease of the ellipse horizontal separation will result in a higher gradient of forces, improving the sensitivity. On the other hand, decrease of the ellipses' size will lead to a lower gradient. Preliminary calculations (numerical integration of interaction between ellipses) show, that with scaling down the ellipses length and width, horizontal separation, and vertical displacement by factor of 5, the gradient of force increased approximately 5 times. This indicates that scaling structure down will not decrease the sensitivity, if the horizontal separation is decreased simultaneously. The presented technology (FIB) allows to decrease the distance between magnetic objects on cantilever to approximately 100 nm (5 times lower than presented in our work).

Since only one cantilever is oscillating, we don't expect that increasing the separation of resonance peaks would influence the phase shift. Additional effect could arise when separation of resonant peaks would be smaller. In that case, the frequency locking of two cantilevers might be present, if the interaction between magnetic elements is strong enough. That could lead to strong change in observed phase and amplitude.

## 5. Conclusions

In summary, in this work we have designed, realized and tested dual-cantilever magnetometer, based on mutual interactions between two micrometer-sized ellipses located on close cantilevers. We have monitored changes in the phase signal of the cantilevers that correspond to different magnetic states in the ellipses (closure-domain state, single-domain state). Observed abrupt change in phase shift has reflected single-domain state flipping of the narrow ellipse.

Furthermore, we have explored magnetic states of the wide ellipse and its influence on the flipping field of the narrow ellipse by changing the direction of the external field. We have shown how to reduce the number of possible magnetic states of the wide ellipse by fixing the local chiralities and vortex polarity. This resulted in significant sharp peak – controlled preferential value of switching field of the narrow ellipse.

For comparison, we have explored magnetic states of the system using MFM and micromagnetic simulations. Simulated hysteresis paths are in agreement with experimental measurements – phase shift and MFM.

It can be concluded, that we have successfully detected magnetic states in ferromagnetic micro elements using the dual-cantilever magnetometer. Experiments were done in the standard commercial AFM microscope with the relative stiff cantilever under ambient conditions without the need for building special equipment or use of an ultrathin cantilever of complicated design. The magnetometer can be improved and it can be applied in experiments on vortex dynamics in the near future.

In the designed dual-cantilever system, the phase shift signal reflects changed interaction between two close cantilevers. Generally, the interaction can be represented not only by magnetic, but also by electric or van der Waals forces, or by chemical bonds or biological chains.

## Acknowledgement

This work was supported by Structural Funds of the European Union by means of the Research Agency of the Ministry of Education, Science, Research and Sport of the Slovak republic in the project "CENTE II" ITMS code 26240120019 and by Slovak Grant Agency APVV, project APVV-0088-12, and by VEGA project 2/0183/15.

## References

[1] Y.P. Hsieh, Z.H. Wei, M.C. Yip, Jap. J. Appl. Phys. 50 (2011) 106601, http://dx.doi.org/10.1143/JJAP.50.106601.
[2] J. Moreland, A. Jander, J.A. Beall, P. Kabos, S.E. Russek, IEEE Trans. Magn. 37 (2001) 2770, http://dx.doi.org/10.1109/20.951302.
[3] T.N. Ng, N.E. Jenkins, J.A. Marohn, IEEE Trans. Magn. 42 (2006) 378, http://dx.doi.org/10.1109/TMAG.2006.870259.
[4] H. Lavenant, V. Naletov, O. Klein, G. de Loubens, L. Casado, J.M. de Teresa, Nanofabrication 1 (2014) 65, http://dx.doi.org/10.2478/nanofab-2014-0006.
[5] L. Bossoni, P. Carretta, M. Poggio, Appl. Phys. Lett. 104 (2014) 182601, http://dx.doi.org/10.1063/1.4874979.
[6] J. Jang, R. Budakian, Y. Maeno, Appl. Phys. Lett. 98 (2011) 132510, http://dx.doi.org/10.1063/1.3572026.
[7] A.C. Bleszynski-Jayich, W.E. Shanks, B. Peaudecerf, E. Ginossar, F. Von Oppen, L. Glazman, J.G.E. Harris, Science 326 (2009) 5950, http://dx.doi.org/10.1126/science.1178139.
[8] N.E. Jenkins, L.P. DeFlores, J. Allen, T.N. Ng, S.R. Garner, S. Kuehn, J.M. Dawlaty, J.A. Marohn, J. Vac. Sci. Tech. B 22 (2004) 909, http://dx.doi.org/10.1116/1.1695336.
[9] S. Lee, E.W. Moore, S.A. Hickman, J.G. Longenecker, J.A. Marohn, J. Appl. Phys. 111 (2012) 083911, http://dx.doi.org/10.1063/1.3699363.
[10] J. Fassbender, J. McCord, J. Magn. Magn. Mater. 320 (2008) 579, http://dx.doi.org/10.1016/j.jmmm.2007.07.032.
[11] C.A. Ross, Annu. Rev. Mater. Res. 31 (2001) 203, http://dx.doi.org/10.1146/annurev.matsci.31.1.203.
[12] V.L. Mironov, O.L. Ermolaeva, E.V. Skorohodov, IEEE Trans. Magn. 52 (2016) 1100607, http://dx.doi.org/10.1109/TMAG.2016.2564947.

[13] V. Novosad, M. Grimsditch, J. Darrouzet, J. Pearson, S.D. Bader, V. Metlushko, K. Guslienko, Y. Otani, H. Shima, K. Fukamichi, Appl. Phys. Lett. 82 (2003) 3716, http://dx.doi.org/10.1063/1.1577808.

[14] J.L. Webb, D. Atkinson, J. Appl. Phys 103 (2008) 033905, http://dx.doi.org/10.1063/1.2837062.

[15] R.P. Cowburn, M.E. Welland, Science 287 (2000) 1466, http://dx.doi.org/10.1126/science.287.5457.1466.

[16] S. Hankemeier, R. Fromter, N. Mikuszeit, D. Stickler, H. Stillrich, S. Putter, E.Y. Vedmedenko, H.P. Oepen, Phys. Rev. Lett. 103 (2009) 147204, http://dx.doi.org/10.1103/PhysRevLett. 103.147204.

[17] L. Gao, D.Q. Feng, L. Yuan, T. Yokota, R. Sabirianov, S. Liou, J. Moreland, J. Appl. Phys. 95 (2004) 7010, http://dx.doi.org/10.1063/1.1682912.

[18] L. Yuan, L. Gao, R. Sabirianov, S.H. Lioun, M.D. Chabot, D.H. Min, J. Moreland, B. Han, IEEE Trans. Magn. 42 (2006) 3234, http://dx.doi.org/10.1109/TMAG.2006.878424.

[19] A. Vansteenkiste, J. Leliaert, M. Dvornik, M. Helsen, F. Garcia-Sanchez, B. Van Waeyenberge, AIP Adv. 4 (2014) 107133, http://dx.doi.org/10.1063/1.4899186.

[20] A. Hubert, R. Schäfer, Magnetic Domains: The Analysis of Magnetic Microstructures, Springer Science & Business Media, 2008.

[21] C.C. Chang, Y.C. Chang, W.S. Chung, J.C. Wu, Z.H. Wei, M.F. Lai, C.R. Chang, IEEE Trans. Magn. 41 (2005) 947, http://dx.doi.org/10.1109/TMAG.2004.842131.

[22] S. Felton, K. Gunnarsson, P.E. Roy, P. Svedlindh, A. Quist, J. Mag. Mag. Mater. 280 (2) (2004) 202, http://dx.doi.org/10.1016/j.jmmm.2004.03.013.

[23] N.A. Usov, C.R. Chang, Z.H. Wei, J. Appl. Phys. 89 (11) (2001) 7591, http://dx.doi.org/10.1063/1.1357133.

[24] www.spmtips.com/afm-tip-hq-nsc35-tipless-no-al.

[25] B. Voigtländer, Scanning Probe Microscopy: Atomic Force Microscopy and Scanning Tunneling Microscopy, Springer, 2015.

[26] V. Cambel, G. Karapetrov, Phys. Rev. B 84 (2011) 014424, http://dx.doi.org/10.1103/PhysRevB.84.014424.

[27] J. Tóbik, V. Cambel, G. Karapetrov, Phys. Rev. B 86 (2012) 134433, http://dx.doi.org/10.1103/PhysRevB.86.134433.

[28] J. Tóbik, V. Cambel, G. Karapetrov, Sci. Rep. 5 (2015) 12301, http://dx.doi.org/10.1038/srep12301.

[29] R. Sandberg, K. Mølhave, A. Boisen, W. Svendsen, J. Micromech. Microeng. 15 (12) (2005) 2249, http://dx.doi.org/10.1088/0960-1317/15/12/006.

[30] K.Y. Yasumura, T.D. Stowe, E.M. Chow, T. Pfafman, T.W. Kenny, B.C. Stipe, D. Rugar, J. Micromech. Sys. 9 (1) (2000) 117, http://dx.doi.org/10.1109/84.825786.